Transient field fluctuations effects in d+Au and Au+Au collisions at $\sqrt{s_{NN}} = 200$ GeV

V. Topor Pop,[1] M. Gyulassy,[2,3] J. Barrette,[1] C. Gale,[1] S. Jeon,[1] and R. Bellwied[4]

[1]*McGill University, Montreal, Canada, H3A 2T8*
[2]*Physics Department, Columbia University, New York, New York 10027, USA*
[3]*Frankfurt Institute for Advanced Studies, J. W. Goethe Universität, D-60438 Frankfurt am Main, Germany*
[4]*Wayne State University, Detroit, Michigan 48201, USA*

The effect of fluctuations of strong color electric fields (SCF) on the baryon production in d+Au and Au+Au collisions at 200A GeV is studied in the framework of the HIJING/B$\bar{\text{B}}$ v2.0 model. It is shown that the dynamics of the production process deviates considerably from calculations based on Schwinger-like estimates for homogeneous and constant color fields. An increase of the string tension from $\kappa_0 = 1$ GeV/fm, to *in medium mean values of* 1.5 to 2.0 GeV/fm and 2.0 to 3.0 GeV/fm for d+Au and Au+Au, respectively, results in a consistent description of the observed nuclear modification factors $R_{d\text{Au}}$ and R_{AuAu} [that relates (d)Au+Au and p+p collisions], and point to the relevance of fluctuations of transient color fields. The differences between nuclear modification factors R_{AuAu} and R_{CP} (that relates central and peripheral collisions) are also discussed. The measurement of multistrange (anti)hyperons (Ξ, Ω) yields would provide a crucial test of the importance of SCF fluctuations at RHIC energies.

PACS number(s): 25.75.Dw, 24.10.Lx

I. INTRODUCTION

While the phase transition from hadronic degrees of freedom to partonic degrees of freedom (quarks and gluons) in ultrarelativistic nuclear collisions is a central focus of recent experiments at the Relativistic Heavy Ion Collider (RHIC), data on baryon and hyperon production have revealed interesting and unexpected features that may be of novel dynamical origin. As an example, a *baryon/meson anomaly* [1–4] is observed as a large enhancement of the baryon to meson ratio and as a large difference of the nuclear modification factor (NMF) between total charged [5] and neutral pions (π^0) [6] at moderate (intermediate) transverse momenta ($2 < p_T < 6$ GeV/c).

In previous papers [7,8] we studied the possible role of topological baryon junctions, [7,9], and the effects of strong color field (SCF) [8] in nucleus-nucleus collisions. We have shown, in the framework of HIJING/B$\bar{\text{B}}$ v2.0 model, that junction-antijunction ($J\bar{J}$) loops with an enhanced *intrinsic transverse momentum* $k_T \approx 1$ GeV/c, a default string tension $\kappa_0 = 1$ GeV/fm, and a diquark suppression factor ($\gamma_{qq} = 0.07$) provide a partial explanation of the baryon/meson anomaly [7]. That model provides an alternative dynamical explanation of the data to recombination models [10]. Within HIJING/B$\bar{\text{B}}$ v2.0 [7,8] one of the main assumptions is that strings could survive and fragment [11,12], and in particular populate the mid to low p_T range. In contrast, in the recombination picture [10] or in the hydrodynamical approach [13] all coherent strings are assumed to become rapidly incoherent resulting in a rapid thermalization.

In nucleus-nucleus collisions the color charge excitations may be considerably greater than in nucleon-nucleon collisions due to the almost simultaneous interaction of several participating nucleons in a row [11,14] and could be important even in the case of few binary collisions. Molecular dynamics models have been used to study the effects of color ropes as an effective description of the nonperturbative, soft gluonic part of QCD [15].

Recently, the effects of gluon field generated in the wake of hard processes and through primordial fluctuations of the color charges in the nuclei have been investigated [16–18]. The physical situation immediately after the collision bears close analogy to string models of high energy collisions. It was shown that the initial electric and magnetic fields produced in high energy hadronic collisions are longitudinal and leads to a novel string-like description of the collisions and a large topological charge density after the collisions [17]. In our model, HIJING/B$\bar{\text{B}}$ v2.0, there are longitudinal electric fields induced by a collision, which subsequently decay by quantum pair production. The effects of longitudinal magnetic fields are taken into account by a specific (like *Mercedes star*) topology for junction antijunction $J\bar{J}$ loops [19]. Strangeness enhancement [20–25], strong baryon transport [8,26], and increase of intrinsic k_T [15] are all expected consequences of SCF. These are modeled in our microscopic models as an increase of the effective string tension that controls the quark-antiquark ($q\bar{q}$) and diquark-antidiquark (qq$\overline{\text{qq}}$) pair creation rates and the strangeness suppression factors [14].

In previous studies [7,8] we have focused on longitudinal rapidity distributions and transverse mass (or momentum) spectra of hadrons and hyperons in Au+Au collisions at RHIC energies. However, the benchmark test of microscopic models are p+p and $p(d) + A$ data. The results from p+p collisions are used as a base line reference to obtain nuclear modification factor R_{AA}. Therefore, we explore further dynamical effects associated with long range coherent fields [i.e., strong color fields (SCF)], including baryon junctions [9] and loops [8,27,28], in the framework of HIJING/B$\bar{\text{B}}$ v2.0 [29], with emphasis on the novel baryon and hyperon observables measured at RHIC in p+p and d+Au collisions. Using this model we analyze baryon/meson anomaly, the

particle species dependence, centrality dependence in d+Au and Au+Au collisions, as well as the differences seen in nuclear modification factors R_{AA} (that relate Au+Au and p+p collisions) and R_{CP} (comparing central and peripheral collisions). Comparison of NMF in different collision systems should provide information on the hadronization mechanisms.

The paper is organized as follows. In Sec. II we review the HIJING/B$\bar{B}$ v2.0 (with SCF) model. For clarity, we repeat here some of the basics outline that has been already presented in Refs. [7,8]. In Sec. III we discuss theoretical predictions in comparison with recent RHIC experimental data. Finally summary and conclusions are given in Sec. IV.

II. HIJING/B$\bar{B}$ V2.0 MODEL

A. Junction antijunction loops

HIJING is a model that provides a theoretical framework to extrapolate elementary proton-proton multiparticle phenomena to complex nuclear collisions as well as to explore possible new physics such as energy loss and gluon shadowing [30]. Our analysis are performed in the framework of the HIJING/B$\bar{B}$ v2.0 model that is based on HIJING/B$\bar{B}$ v1.10 [27,28] and HIJING [30].

In HIJING [30] the soft beam jet fragmentation is modeled by diquark-quark strings as in [31] with gluon kinks induced by soft gluon radiations. The minijet physics is computed via an eikonal multiple collision framework using pQCD PYTHIA 7.3 to compute the initial and final state radiation and hard scattering rates. In PYTHIA the cross section for hard parton scatterings is enhanced by a factor $K = 2$ in order to simulate high order corrections. HIJING extends PYTHIA to include a number of new nuclear effects. Besides the Glauber nuclear eikonal extension, shadowing of nuclear parton distributions is modeled. In addition dynamical energy loss of the (mini)jets is taken into account through an effective energy loss, dE/dx [30,32].

In HIJING/B$\bar{B}$ v1.10 [27] the baryon junction mechanism was introduced as an extension of HIJING/B [33] in order to try to account for the observed longitudinal distributions of baryons (B) and antibaryons ($\bar{B}$) in proton nucleus (p+A) and nucleus-nucleus ($A + A$) collisions at the SPS energies. However, as implemented in HIJING/B$\bar{B}$ v1.10, the junction loops fails to account for the observed enhanced transverse slope of antibaryons spectra at moderate p_T in $A + A$ [32]. This is due to limitations of the p_T algorithm adopted in version 1.10 that includes kinematic constraints that worked to oppose the predicted enhancement in the baryon junction loop [9]. In HIJING/B$\bar{B}$ v2.0 we replaced that algorithm with one that implements $J\bar{J}$ loops p_T enhancement directly. This is done by specifying the intrinsic (anti)diquark p_T kick in any standard diquark-quark string (qq-q) that contains one or multiple $J\bar{J}$ loops. In addition, we introduced a new formula [see Eq. (1) below] for generating the probability that a given diquark or antidiquark gets an "*enhanced p_T kick*" from the underlying junction mechanism. We emphasize that while there is very strong evidence from a variety of data that the source of the observed baryon p_T enhancement arises more naturally from collective hydrodynamic flow [13], elliptic flow of

heavy hyperons [34] argues strongly for a dominant partonic collective flow as the origin of the baryon anomaly. Most of the initial baryon radial p_T could theoretically arise from the production mechanism, while its elliptic deformation would arise from final state interactions. Nevertheless, our purpose here is to explore more fully without the kinematic limitations of version 1.10, the theoretical problem of how much of the baryon anomaly could be due to the postulated baryon junction dynamics [9] at RHIC energies and how well is described (p)d+Au collisions with emphasis on strangeness production. The details of this new implementation of $J\bar{J}$ loops are described below.

Multiple hard and soft interactions proceed as in HIJING. Before fragmentation, we compute via JETSET [31] the probability that a junction loop occurs in the string. A picture of a junction loop is as follows: a color flux line splits at some intermediate point into two flux lines at one junction and then the flux lines fuse back into one at a second antijunction somewhere further along the original flux line. The distance in rapidity between these points is chosen via a Regge distribution as described below. For single inclusive baryon observables this distribution does not need to be specified.

The probability of such a loop is assumed to increase with the number of binary interactions, n_{hits}, that the incident baryon suffers in passing through the oncoming nucleus. This number depends on the relative and absolute impact parameters and is computed in HIJING using the eikonal path through a diffuse nuclear density.

We assume that out of the nonsingle diffractive NN interaction cross section, $\sigma_{nsd} = \sigma_{in} - \sigma_{sdf}$, a fraction of events $f_{J\bar{J}} = \sigma_{J\bar{J}}/(\sigma_{in} - \sigma_{sdf})$ excite a junction loop (where σ_{sdf} is single diffractive cross sections). The probability after n_{hits} that the incident baryon has a $J\bar{J}$ loop is

$$P_{J\bar{J}} = 1 - (1 - f_{J\bar{J}})^{n_{hits}}. \tag{1}$$

We take $\sigma_{J\bar{J}} = 17$ mb, $\sigma_{sdf} \approx 10$ mb, and $\sigma_{in} \approx 42$ mb for the total inelastic nucleon-nucleon cross section at nucleon-nucleon (NN) center of mass (c.m.) energy $\sqrt{s_{NN}} = 200$ GeV. These cross sections imply that at $\sqrt{s_{NN}} = 200$ GeV, a junction loop occurs in p+p collisions with a rather high probability $17/32 \approx 0.5$ and rapidly approaches 1 in $A + A$ collisions. In $p + S$ where $n_{hits} \approx 2$ there is an 80% probability that a junction loop occurs in this scheme. Thus the effects of loops is taken here to have a very rapid onset and essentially all participant baryons are excited with $J\bar{J}$ loops in $A + A$ collisions at RHIC. However, the actual probability is modified by string fragmentation due to the threshold cutoff mass $M_c = 6$ GeV, which provides sufficient kinematical phase space for $B\bar{B}$ pair production. We investigated the sensitivity of the results to the value of parameters $J\bar{J}$ and found no significant variation on pseudorapidity distributions of charged particles produced in Au+Au collisions at $\sqrt{s_{NN}} = 200$ GeV, assuming cross sections $\sigma_{J\bar{J}}$, 15 mb $< \sigma_{J\bar{J}} < 25$ mb and a cutoff mass M_c, 4 GeV $< M_c < 6$ GeV. Light ion reactions such as, p+A or d+Au should show more sensitivity to $\sigma_{J\bar{J}}$.

In HIJING/B$\bar{B}$ v2.0, we introduced [7] the possible topology with two junctions [19] and a new algorithm where $J\bar{J}$ loops are modeled by an enhancing diquark p_T kick characterized by a Gaussian width of $\sigma'_{qq} = f \cdot \sigma_{qq}$, where f is

a broadening factor, and $\sigma_{qq} = 0.350$ GeV/c (consistent with
PYTHIA [31] default value). In Ref. [7], we concluded that
a value $f = 3$ best reproduced the (anti)proton p_T spectra in
Au+Au collisions at $\sqrt{s_{NN}} = 200$ GeV. This implementation
of the $J\bar{J}$ loops mechanism marks a radical departure from
that implemented in HIJING/B$\bar{\rm B}$ v1.10. While the above
procedure allows baryon antibaryon pairs to acquire much
higher transverse momentum in agreement with observation,
the absolute production rate also depends on the diquark/quark
suppression factor γ_{qq} (see Sec. II B). The factor f modifying
the default value $\sigma_{qq} = 0.350$ GeV/c may depend on beam
energy, atomic mass number (A), and centrality (impact
parameter). However, we will show that a surprising good
description of a variety of observables is obtained with
a constant value, $f = 3$. The sensitivity of the theoretical
predictions to this parameter is discussed in Sec. III. Finally,
we remark that baryon antibaryon correlations studies in $p+p$
and $p(d) +$ Au collisions at RHIC energies could eventually
help us to obtain more precise values of $J\bar{J}$ loops parameters
[mainly: $\sigma_{J\bar{J}}$, Regge intercept $\alpha(0)$, and parameter f].

Phenomenological descriptions are currently based on
Regge trajectory which gives the appropriate relationship
between the mass M of the hadrons and its spin J_s : $J_s =
\alpha(0) + \alpha_s M^2$, where $\alpha(0)$ is the Regge intercept, and α_s is
the Regge slope. The value of the Regge slope for baryons is
$\alpha_s \simeq 1$ GeV^{-2} [28] that yields a string tension (related to the
Regge slope, $\kappa_0 = 1/2\pi\alpha_s$) $\kappa_0 \approx 1.0$ GeV/fm. The multigluon
exchange processes dominated by Pomeron exchange in high
energy nucleus-nucleus collisions could be described by a
Regge trajectory with a smaller slope $\alpha_s' \approx 0.45$ GeV^{-2} [35],
leading to an increase of string tension to $\kappa \approx 2\kappa_0$.

The contribution to the double differential inclusive cross
section for the inclusive production of a baryon and an
antibaryon in NN collisions due to $J\bar{J}$ exchange is given
by [9,27]

$$E_B E_{\bar{B}} \frac{d^6\sigma}{d^3 p_B d^3 p_{\bar{B}}} \rightarrow C_{B\bar{B}} e^{(\alpha(0)-1)|y_B - y_{\bar{B}}|}, \qquad (2)$$

where $C_{B\bar{B}}$ is an unknown function of the transverse
momentum and $M_0^J + P + B$ (junction+Pomeron+baryon)
couplings [27]. The predicted rapidity correlation length
$(1 - \alpha(0))^{-1}$ depends upon the value of the Regge intercept
$\alpha(0)$. A value of $\alpha(0) \simeq 0.5$ [9] leads to rapidity correlations
on the scale $|y_B - y_{\bar{B}}| \sim 2$, while a value $\alpha(0) \simeq 1.0$ [36] is
associated with infinite range rapidity correlations. Thus, it
is important to study rapidity correlations at RHIC energies
where very high statistics data are now available.

B. Strong color field within HIJING/BB̄ v2.0

In the case of quark-gluon plasma (QGP) creation it
is necessary to modify the dynamics of particle vacuum
production at short time scales and the abundance of newly
produced particle may deviate considerably from the values
obtained assuming a constant field [37,38]. Two possible
processes that lead to an increase of strangeness production
within the framework of the Schwinger mechanism are
(i) an increase in the field strength by a modified string tension

κ [14,24,39], or (ii) a drop in the quark masses due to chiral
symmetry restoration [40–43]. A specific chiral symmetry
restoration could be induced by a rapid deceleration of the
colliding nuclei [44].

For a uniform chromoelectric flux tube with field (E) the
probability to create a pair of quarks with mass m, effective
charge ($e_{\rm eff}$), and transverse momentum (p_T) per unit time and
unit volume is given by [45]

$$P(p_T)d^2 p_T$$
$$= -\frac{|e_{\rm eff}E|}{4\pi^3} \ln\left\{ 1 - \exp\left[-\frac{\pi(m^2 + p_T^2)}{|e_{\rm eff}E|} \right] \right\} d^2 p_T. \quad (3)$$

The integrated probability (P_m), when the leading term in
Eq. (3) is taken into account, is given by

$$P_m = \frac{(e_{\rm eff}E)^2}{4\pi^3} \sum_{n=1}^{\infty} \frac{1}{n^2} \exp\left(-\frac{\pi m^2 n}{|e_{\rm eff}E|} \right), \qquad (4)$$

where each term in the sum corresponds to production of
n coherent pairs, and E is an homogeneous electric field,
and $\kappa = |e_{\rm eff}E|$ is the so-called string tension. We note, that
P_m reproduces the classical Schwinger results [46], derived
in spinor quantum electrodynamics (QED) for describing
positron-electron ($e^+ e^-$) production rate. A sizable rate for
spontaneous pair production requires "*strong electric fields*,"
and $|e_{\rm eff}E|/m^2 > 1$.

Recently, nonperturbative gluon and quark-antiquark pair
production from a constant chromoelectric field with arbitrary
color index via vacuum polarization have been also investi-
gated in a QCD formalism [47]. Although the p_T dependence
of the rate of production is different because of the presence
of the nontrivial color generators in QCD, the integration over
p_T, reproduced also Schwinger's result for total production
rate used here to estimate the suppression of heavier flavors.

The real fields emerging in heavy-ion collisions, could be
inhomogeneous, with a space-time dependence. Up to now,
no reliable and universal method is available for calculating
pair production rates in inhomogeneous electric fields (for a
review see Ref. [48]). Different theoretical methods, such as
functional techniques [49] or kinetic equations [37,38] have
been developed. It was shown [49] that the above formula is
a very good approximation in the limit of sufficiently intense
fields if the field does not vary appreciably over space-time
distances of less than $m^{-1}(m^2/|e_{\rm eff}E|)$. In the case of a QGP
creation in heavy-ion collisions, the characteristic time of the
field variation is estimated to be of order of 1 fm/c [13], and
we have to consider a time-dependent homogeneous field.
Taking a soliton-like field, the production probability for
strange quarks is 1.5 times larger than in stationary case [37],
and therefore, the abundance of newly produced multistrange
particles may considerably deviate from the values obtained
for the constant field.

In HIJING/B$\bar{\rm B}$ v2.0, as in HIJING, no attempt has been
made thus far to study possible modifications of Lund
string fragmentation by back reaction effects as discussed in
reference [50]. These effects, important for consideration of
final state interaction kinetic theory, go beyond the scope of
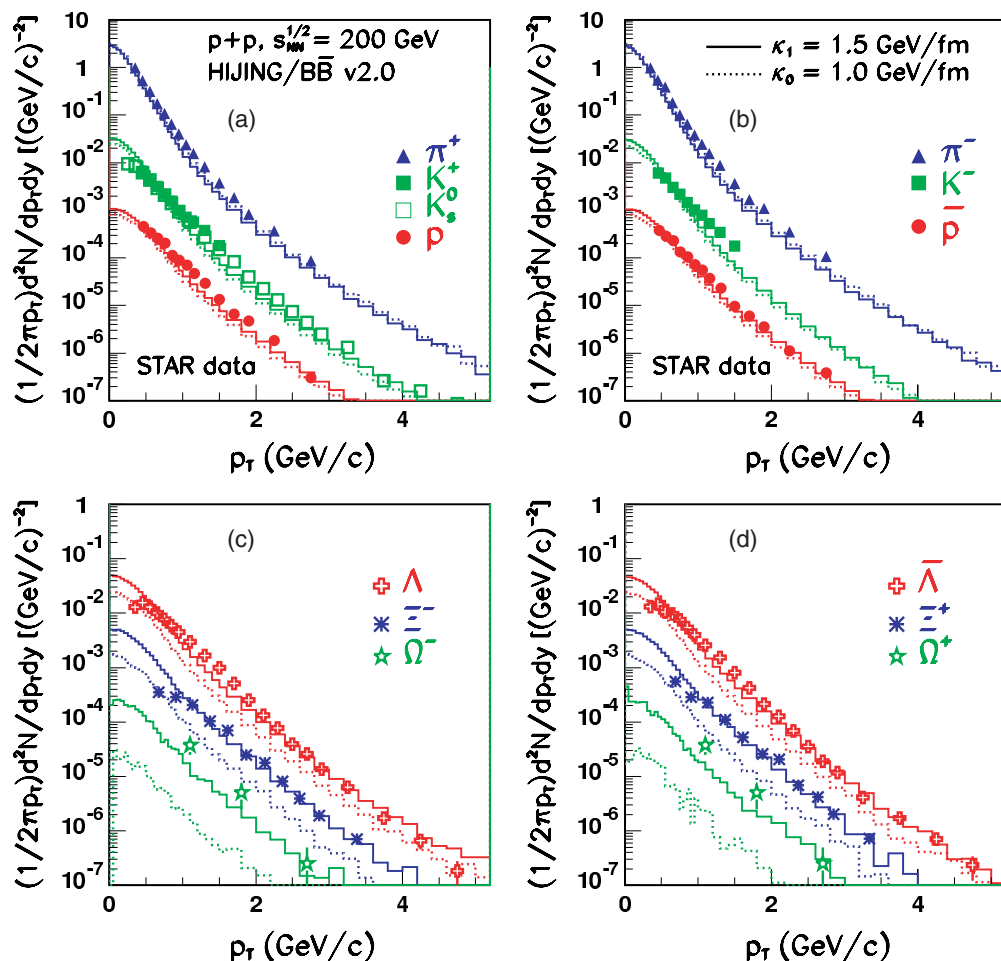the present phenomenological investigation.

FIG. 1. (Color online) Comparison of HIJING/BB̄ v2.0 predictions for the invariant yields of pions, kaons (scaled by 10^{-1}), protons (scaled by 10^{-2}) and their antiparticles (upper panels) and (multi)strange and their antiparticles (lower panels) as function of p_T from nonsingle diffractive (NSD) $p+p$ colllisions at $\sqrt{s_{NN}} = 200$ GeV. The rapidity range was $-0.5 < y < 0.5$. Results with $\kappa_1 = 1.5$ GeV/fm (solid histograms; Table I, set 3) and with $\kappa_0 = 1.0$ GeV/fm (dotted histograms; Table I, set 1) are shown. The data are from STAR [66,67]. Only statistical error bars are shown.

A value for the strength of the external field, based on an estimate of initial energy density of 50 GeV/fm³ at RHIC [51], is $E_{ex} \approx 3.16$ GeV/fm. Due to time dependence and fluctuations of the chromoelectric field at the initial stage of the collision we may even expect higher values. It has been suggested that the magnitude of a typical field strength at maximum RHIC energies might reach 5–12 GeV/fm [26].

In general in microscopic string models the heavier flavors (and diquarks) are suppressed according to Schwinger formula (for homogeneous strong color field, E) [46]:

$$\gamma_Q = \frac{P(Q\bar{Q})}{P(q\bar{q})} = \exp\left(-\frac{\pi\left(m_Q^2 - m_q^2\right)}{\kappa}\right), \qquad (5)$$

where $\kappa = |e_{\text{eff}} E|$ is the *string tension*; m_Q is the effective quark mass; $Q = s$ for strange quark; $Q = qq$ for a diquark, and $q = u, d$ are the light nonstrange quarks.

The main parameters of QCD, the coupling strength α_{QCD} and the quark masses, need to be determined precisely. However, present estimates [52] of the *current quark masses*

range from: $m_u = 1.5$–5 MeV; $m_d = 3$–9 MeV, and $m_s = 80$–190 MeV. For diquark we consider $m_{qq} = 450$ MeV [53]. Taking for constituent quark masses of light nonstrange quark $M_{u,d} = 230$ MeV, strange quark $M_s = 350$ MeV [54], and diquark mass $M_{qq} = 550 \pm 50$ MeV as in Ref. [53], it is obvious that the masses of (di)quark and strange quark will be substantially reduced at the chiral phase transition. If the QGP is a chirally restored phase of strongly interacting matter, in this picture, the production of strange hadrons will be enhanced [42]. In this case, a possible decrease of the strange quark mass would lead to a similar enhancement of the suppression factors, obtained (in microscopic models) by an increase of string tension [37,41]. If the strange quark mass is reduced from $M_s = 350$ MeV to the current quark mass of approximately $m_s \approx 150$ MeV (the actual values are $m_s = 80$–170 MeV, see Ref. [52]), we obtain from Eq. (5) for strangeness suppression factor $\gamma_s^1 \approx 0.70$. For a string tension increase from $\kappa_0 = 1.0$ GeV/fm to $\kappa = 3.0$ GeV/fm, we obtain an identical value $\gamma_s^1 \approx 0.69$. Moreover, if we consider that Schwinger tunneling could explain the thermal character of hadron spectra and that,
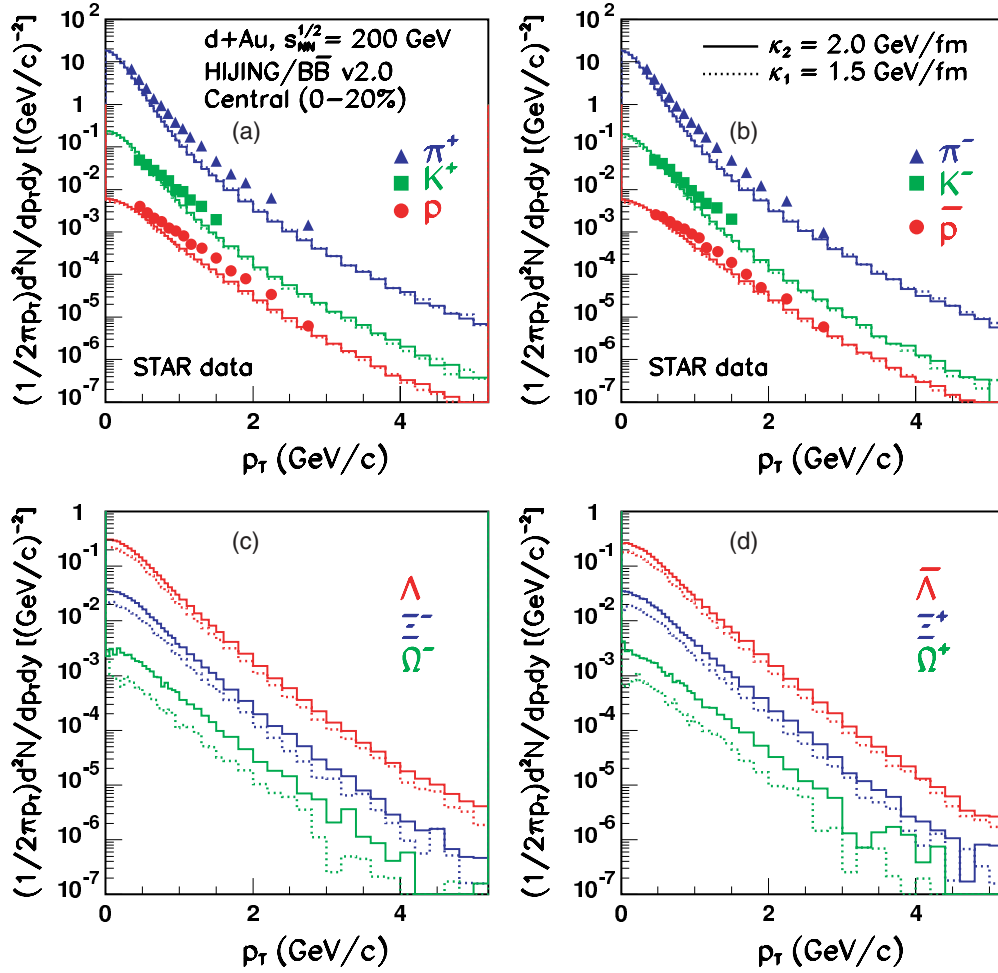
FIG. 2. (Color online) Upper part: comparison of HIJING/B$\bar{\text{B}}$ v2.0 predictions for the invariant yields of pions, kaons (scaled by 10^{-1}), protons (scaled by 10^{-2}) (left panel) and their antiparticles (right panel) as function of p_T for central (0–20%) d+Au collisions at $\sqrt{s_{NN}} = 200$ GeV. Lower part: spectra for strange (Λ) and multistrange (Ξ^-, Ω^-) particles (left panel), and their antiparticles (right panel). The rapidity range was $-0.5 < y < 0.5$. Results with $\kappa_2 = 2.0$ GeV/fm (solid histograms; Table II, set 4) and with $\kappa_1 = 1.5$ GeV/fm (dotted histograms; Table II, set 3) are shown. The data are from STAR [66]. Only statistical error bars are shown.

due to SCF effects, the string tension value κ fluctuates, we can define an apparent temperature as function of the average value of string tension ($\langle\kappa\rangle$), $T = \sqrt{\langle\kappa\rangle/2\pi}$ [55,56].

There is a debate in the study of the qqq system on the relative contribution of the Δ-like geometry and the Y-like geometry [19,57], and on the stability of these configurations for the color electric fields [58]. In both topologies we expect a higher string tension than in an ordinary $q\bar{q}$ string ($\kappa_Y = \sqrt{3}\,\kappa_0$ and $\kappa_\Delta = (3/2)\,\kappa_0$). It was shown [58] that the total string tension has neither the Y nor the Δ-like value, but lies rather in-between the two pictures. However, the Y configuration appears to be a better representation of the baryons. If two of these quarks stay close together, they behave as a diquark [57]. In a dual superconductor models of color confinement for the Y-geometry, the flux tubes converge first toward the center of the triangle and there is also another component which run in the opposite direction (*Mercedes star*). They attract each other and this lower the energy of the Y-configuration [19].

Our calculations are based on the assumption that the effective enhanced string tension (κ), in both, basic ropes

($q^n - \bar{q}^n$) and junction ropes ($q^n - q^n - q^n$) are the same. For elementary n strings and junctions this ansatz is supported by baryon studies [59]. A different approach to baryon production without baryon junctions has been proposed in [24] where SCF from the string fusion process can lead to $(qq)_6 - (\bar{q}\bar{q})_{\bar{6}}$ with about a doubling of the string tension. Both types of SCF configurations may arise but predict different rapidity dependence of the valence baryons.

Following the discussions above, we take into account SCF in our model by an *in medium effective string tension* $\kappa > \kappa_0$, which lead to new values for the suppression factors, as well as the new effective intrinsic transverse momentum k_T. This includes (i) the ratio of production rates of diquark to quark pairs (diquark suppression factor), $\gamma_{qq} = P(qq\overline{qq})/P(q\bar{q})$, (ii) the ratio of production rates of strange to nonstrange quark pairs (strangeness suppression factor), $\gamma_s = P(s\bar{s})/P(q\bar{q})$, (iii) the extra suppression associated with a diquark containing a strange quark compared to the normal suppression of strange quark (γ_{us}), $\gamma_{us} = (P(us\overline{us})/P(ud\overline{ud}))/(\gamma_s)$, (iv) the suppression of spin 1 diquarks relative to spin 0 ones (apart
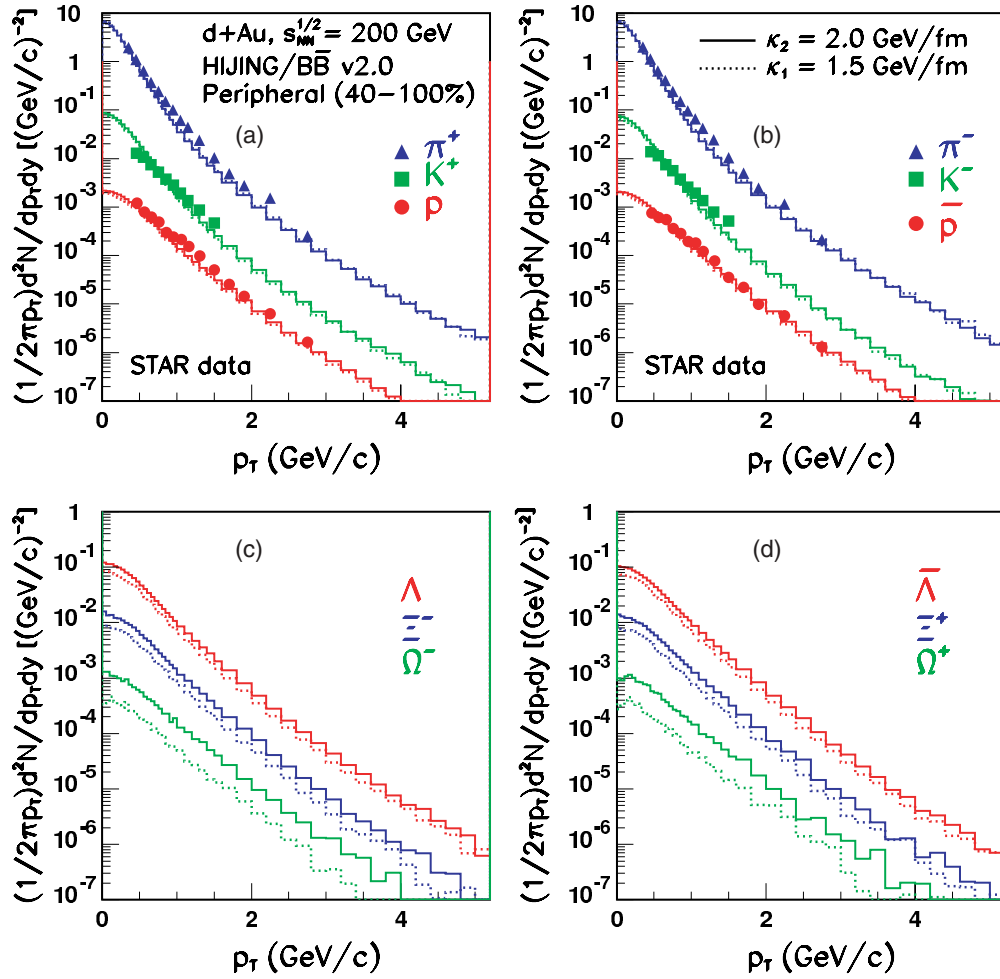
FIG. 3. (Color online) Results for peripheral (40–100%) d+Au colllisions at $\sqrt{s_{NN}} = 200$ GeV. The histograms have the same meaning as in Fig. 2. The data are from STAR [66]. Only statistical error bars are shown.

from the factor of three enhancement of the former based on counting the number of spin states), γ_{10}, and (v) the (anti)quark ($\sigma_q'' = \sqrt{\kappa/\kappa_0} \cdot \sigma_q$) and (anti)diquark ($\sigma_{qq}'' = \sqrt{\kappa/\kappa_0} \cdot f \cdot \sigma_{qq}$) Gaussian width. These parameters correspond to $\gamma_{qq} =$ PARJ(1), $\gamma_s =$ PARJ(2), $\gamma_{us} =$ PARJ(3), $\gamma_{10} =$ PARJ(4), and $\sigma_{qq} = \sigma_q =$ PARJ(21) of the JETSET subroutines [31]. The values of the main parameters sets used in our analysis (i.e., f, σ_q, as well as the suppression factors γ_{qq}, γ_s, γ_{us}, and γ_{10}) are found in the Appendix.

III. NUMERICAL RESULTS

A. Transverse momentum spectrum

1. Identified particles spectra from $p+p$ collisions at $\sqrt{s_{NN}} = 200$ GeV

We will concentrate our discussions on species dependence of the nuclear modification factors (NMFs) R_{AA} and R_{CP} in d+Au and Au+Au collisions at $\sqrt{s_{NN}} = 200$ GeV. R_{AA} is the ratio of the heavy-ion yield to the pp cross section normalized by the mean number of binary collisions ($\langle N_{\rm bin} \rangle$), while R_{CP} is the ratio of scaled central to peripheral particle

yield. They are defined as in Ref. [7]. By comparing the yields in $p(d) + A$ and $A + A$ collisions to that from $p+p$ collisions, with a scaling factor to take into account the nuclear geometry, one can test the assumption that nucleus-nucleus collision is a simple superposition of incoherent nucleon-nucleon scattering and explore possible nuclear effects (e.g., shadowing, quenching, SCF). The relevance of baseline $p+p$ hard p_T spectra for understanding high-energy nucleus-nucleus physics is discussed in Ref. [60]. The precision in the first results on NMFs R_{AA}, were limited by the uncertainty in the parametrization of the $p+p$ reference spectrum used in obtaining R_{AA}. This limitation was partly overcome when new data on $p+p$, d+Au and Au+Au collisions at $\sqrt{s_{NN}} = 200$ GeV using the same experimental setup were obtained [61–72].

Before discussing our results on the NMFs that are scaled yield ratios, it is important to show how well the model describe $p+p$ collision data. Figure 1 presents a comparison of experimental transverse momentum spectra [66,67] of positive pions (π^+), kaons (K^+), protons (p), (multi)strange particles and their antiparticles, with the predictions of regular HIJING (dotted histograms) and HIJING/B$\bar{\rm B}$ v2.0 (solid histograms). HIJING results describe rather well the data for produced
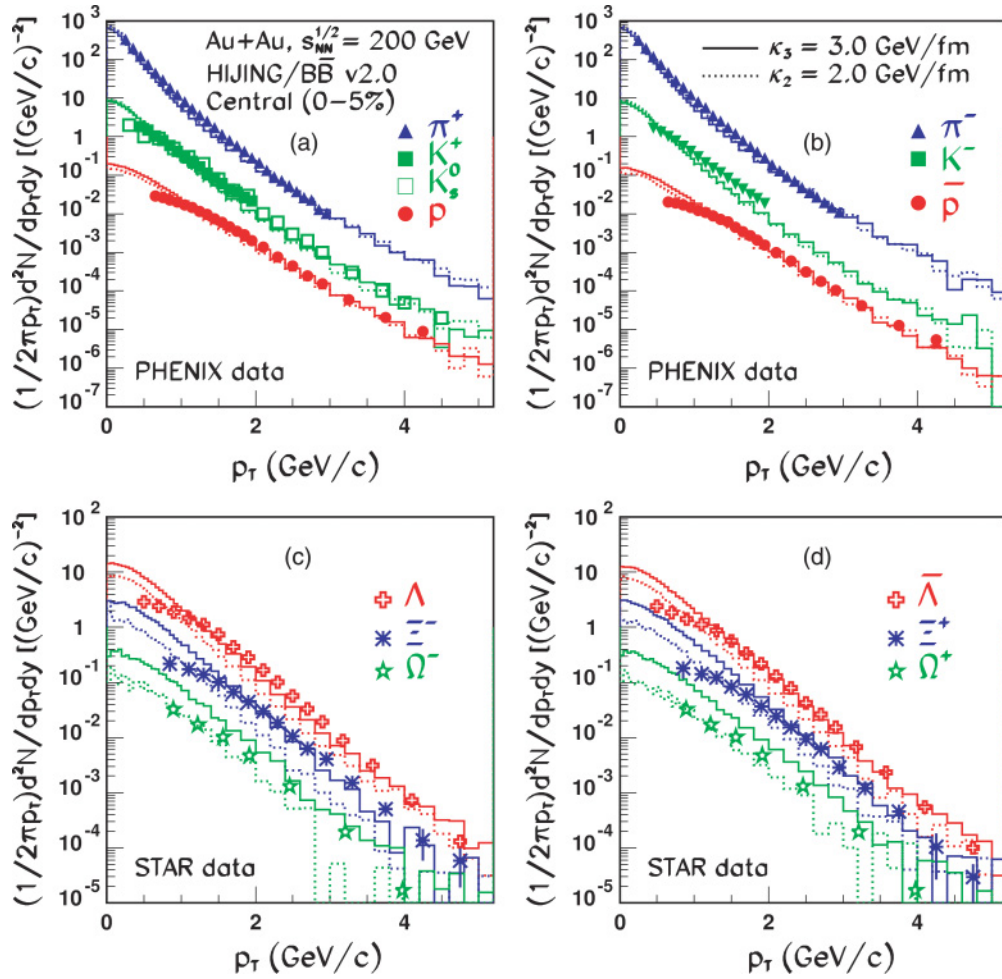
FIG. 4. (Color online) Upper part: comparison of HIJING/B$\bar{\text{B}}$ v2.0 predictions for the invariant yields of pions, kaons (scaled by 10^{-1}), protons (scaled by 10^{-2}) (left panel) and their antiparticles (right panel) as function of p_T for central (0–5%) Au+Au colllisions at $\sqrt{s_{NN}} = 200$ GeV. Lower part: spectra for strange (Λ) and multistrange (Ξ^-, Ω^-) particles (left panel), and their antiparticles (right panel). The rapidity range was $-0.5 < y < 0.5$. Results with $\kappa_3 = 3.0$ GeV/fm (solid histograms; Table II, set 5) and with $\kappa_2 = 2.0$ GeV/fm (dotted histograms; Table II, set 4) are shown. The data are from PHENIX [69] and STAR [70,71]. Only statistical error bars are shown.

"bulk particles" (i.e., pions, protons, and kaons). We would have expected that other (multi)strange particles to also be well described by the standard fragmentation included in HIJING, since the universality of the fragmentation process between positron-electron ($e^+ + e^-$) and $p+p$ collisions has been confirmed [76]. However, regular HIJING underestimate significantly the spectra of lambda and cascade particles (Figs. 1(c) and 1(d)).

HIJING/B$\bar{\text{B}}$ v2.0 results include the contribution of a broadening of the intrinsic momentum (k_T), simulated by an increase of the string tension from the default value $\kappa_0 = 1.0$ GeV/fm (Table I, set 2) to $\kappa_1 = 1.5$ GeV/fm (Table I, set 3). Such parametrization is supported by earlier experimental measurements [73], showing that at center of mass energy $\sqrt{s_{NN}} > 100$ GeV, collisions between protons and antiprotons, largely consist of more than a single parton-parton interaction. It is also supported by a recent PHENIX analysis of the properties of jets produced in $p+p$ collisions at $\sqrt{s_{NN}} =$

200 GeV [74], giving a value of $\langle k_T \rangle = 1.34 \pm 0.04 \pm 0.29$ GeV/c, much larger than the naive expectation for the pure intrinsic parton transverse momentum based on nucleon constituent quark mass (i.e., $\langle k_T \rangle \approx 0.300$ GeV/c) [75]. This new parametrization results in an increase of the yield of (multi)strange particles without affecting significantly results for the "bulk particles" and thus gives a simultaneous description of the nonstrange and multi-strange sector.

A related approach has been recently presented by STAR collaboration [68]. They introduced an improved description for strange particles using PYTHIA by increasing the K factor which quantifies the contributions of next-to-leading order (NLO) effects, from $K = 2$ to $K = 3$. We test this suggestion using our model and observes that such increase of K results in an overestimation of pions, kaons, and protons yields. In our calculations we keep K to its default value in PYTHIA and HIJING i.e., $K = 2$ for all collisions.
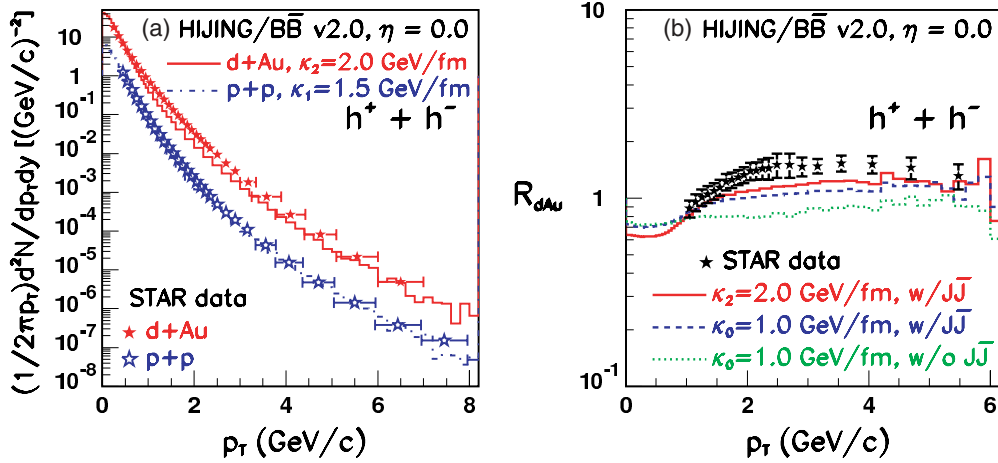
FIG. 5. (Color online) Left panel: HIJING/B$\bar{\rm B}$ v2.0 predictions with SCF for p_T spectra at midrapidity of total inclusive charged hadrons, for central (0–20%) d+Au and p+p collisions. The calculations assume $\kappa_2 = 2.0$ GeV/fm for d+Au (solid histograms; Table II, set 3) and $\kappa_1 = 1.5$ GeV/fm for p+p (dot-dashed histograms; Table I, set 3). Right panel: Nuclear modification factor $R_{d\rm Au}$. The results obtained without $J\bar{J}$ loops and SCF (dotted; Table II, set 1), including only $J\bar{J}$ loops (dashed; Table II, set 2), and including both effects $J\bar{J}$ loops and SCF (solid histograms, Table II, set 3) are shown. The data are from STAR [63,78]. Only statistical error bars are shown.

2. Identified particles spectra from d+Au collisions at $\sqrt{s_{NN}} = 200\,GeV$

Initial-state nuclear effects are present in both d+Au and Au+Au collisions, while final state effects are expected to contribute only in Au+Au collisions. Thus, effects from the initial state are best studied through a "control" experiment such as d+Au collisions [77–80]. Multiple soft scattering of projectile partons as they traverse a target nucleus may increase their transverse momentum before they undergo the hard scattering or subsequent to it, leading to an enhancement of the yield at moderate and high p_T compared to p+p collisions—called the Cronin effect [81,82]. This enhancement is expected to have some particle mass dependence and to be stronger for

heavier particles [82]. The Cronin enhancement was addressed in Refs. [83–86]. However, these pQCD calculations cannot predict the particle species dependence observed in the data, as initial state parton scattering precedes fragmentation into the different hadronic species. An alternative explanation considering final state interactions is discussed in Ref. [90].

HIJING type models incorporate in addition to the soft and hard dynamics (discussed in Sec. II A) a simulation of soft multiple initial state collision effects [91]. Excited strings are assumed to pick up random transfer momentum kicks in each inelastic scattering according to the distribution:

$$g(k_c) \propto \left\{ \left(k_c^2 + p_1^2\right)\left(k_c^2 + p_2^2\right)(1 + \exp[(k_c - p_2)/p_3]) \right\}^{-1},$$
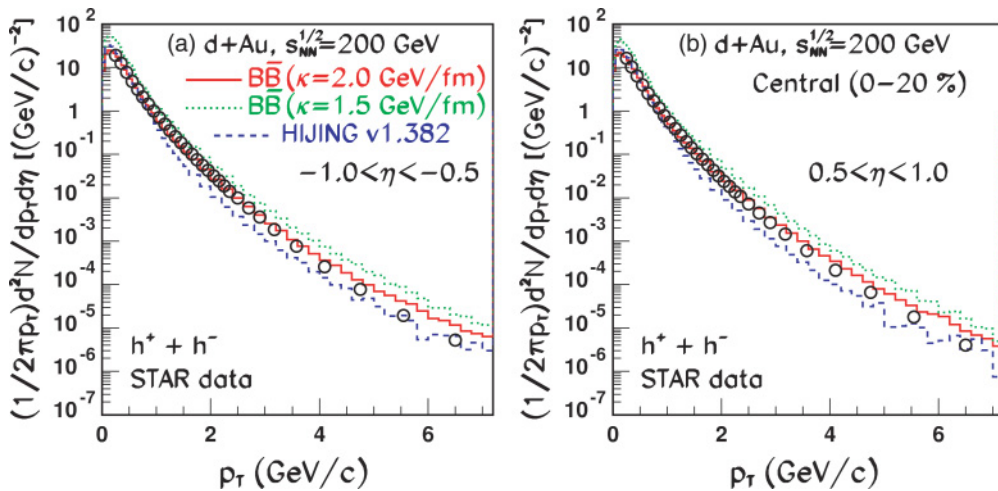
$$(6)$$

FIG. 6. (Color online) HIJING/B$\bar{\rm B}$ v2.0 (with SCF) and HIJING v1.382 predictions for p_T spectra of total inclusive charged hadrons, for central (0–20%) d+Au collisions, in backward ($-1.0 < \eta < -0.5$, left panel) and forward ($0.5 < \eta < 1.0$, right panel) pseudorapidity region. The calculations assume $\kappa_2 = 2.0$ GeV/fm for d+Au (solid histograms; Table II, set 4) and $\kappa_1 = 1.5$ GeV/fm for dotted histograms; Table II, set 3). The dashed histograms are the results obtained within HIJING v1.382, with default parameters. The calculations in both models are obtained with shadowing and without jet quenching. The data are from STAR [96]. Only statistical error bars are shown.
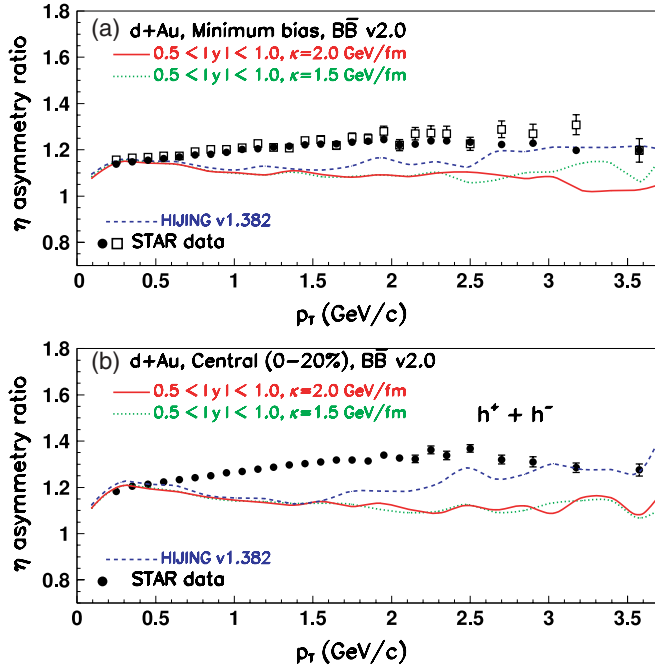
FIG. 7. (Color online) The ratio of charged hadron spectra in the backward rapidity to forward rapidity region for minimum bias (upper panel) and central (0–20%) (lower panel) d+Au collisions. The curves have the same meaning as in Fig. 6. The data are from STAR [96]. Only statistical error bars are shown.

where k_c represents the intrinsic transverse momentum of the colliding partons. The parameters $p_1 = 0.1$, $p_2 = 1.4$, $p_3 = 0.4$ GeV/c are chosen to fit the low energy multiparticle production [30]. A flag in the code makes it possible to compute spectra with and without this effect. At RHIC energies the observed larger enhancement for protons and antiprotons in comparison with pions [72] requires new processes beyond the initial state multiple scattering. In addition to "Cronin enhancement" other known initial state effects that could contribute include nuclear shadowing [30,87,88], gluon saturation [89], $J\bar{J}$ loops, and SCF effects Ref. [8].

In order to further understand the mechanisms responsible for the particle p_T spectra, and to separate the effects of initial and final partonic rescatterings we study the transverse momentum spectra at midrapidity of identified particles in central (0–20%) (Fig. 2) and peripheral (40–100%) (Fig. 3) d+Au collisions. The data are compared to the predictions of our model assuming two values of the string tension, $\kappa_2 = 2.0$ GeV/fm (solid histograms) and $\kappa_1 = 1.5$ GeV/fm (dotted histograms). All calculations include nuclear shadowing but do not take into consideration "jet quenching," since d+Au collisions create a "cold nuclear medium." The agreement above 1 GeV/c, is very good for peripheral ($\langle N_{bin} \rangle = 4.5$) and minimum bias ($\langle N_{bin} \rangle = 7.8$) events (not shown here). Within our model the observed "Cronin enhancement" for identified particle spectra at moderate p_T, as well as species dependence, are satisfactorily predicted at midrapidity due to a subtle interplay of initial state effects.

However, the calculations somewhat underestimate the pion, proton, and kaon yield in the case of central d+Au

collisions ($\langle N_{bin} \rangle = 14.8$). To quantify the competing mechanisms contributing to the particle yield, we study in the above results, the contribution from "soft Cronin" and shadowing effects. Including "soft Cronin" through Eq. (6) results in an increase of the yield which is higher for protons ($\approx$40% for $p_T = 2$–3 GeV/c) than for pions ($\approx$20%, for $p_T = 2$–3 GeV/c). On the other hand, shadowing effects result in a roughly equal decrease of the yield of all species, i.e., $\approx$25% in the same p_T region. Therefore, these two effects act in opposite directions and partly cancel each other at low and moderate p_T ($<$5 GeV/c). In addition, we cannot improve the overall description of p_T spectra, by modifying the parameters from Eq. (6), without destroying the satisfactory results at low p_T (0.0–1.5 GeV/c). A further increase of mean values of string tension to values greater than 2.0 GeV/fm, results in a stronger underestimation of the pions yields. The description of p_T spectra for central collisions point to a mechanism not included in our model. The disagreement may be explained by considering hadronic rescattering in gold nucleus as in Multi Phase Transport (AMPT) model [92], or inelastic and elastic parton ladder splitting as in EPOS model [93]. We do not include here a discussion of the particle production at forward rapidity, where possible gluon saturation effects (color glass condensate CGC) [89] or parton ladder splitting [93], may have to be considered.

In Sec. III B we will discuss the nuclear modification factor for (multi)strange particles. Therefore, predictions for Λ, Ξ^-, Ω^- and their antiparticles are also shown in Figs. 2 and 3 (lower panels) for the same centrality selections. We note that in d+Au collisions the sensitivity to in medium string tension depend on mass and strangeness content, resulting in a predicted significant increase of the yield of multi-strange hyperons (Ξ and Ω).

3. Identified particles spectra from Au+Au collisions at $\sqrt{s_{NN}} = 200$ GeV

Figure 4 presents a comparison of the transverse momentum spectra of identified π^+, K^+, and p and their antiparticles with the predictions of HIJING/B$\bar{B}$ v2.0 (upper panels) for central (0–5%) Au+Au collisions. These data are taken from Ref. [69]. A similar comparison (lower panels) is also presented for Λs (for central 0–5%), Ξ^-s, Ω^-s (for central 0–10%) and their antiparticles. These data are taken from Ref. [71]. The shape of the measured spectra show a clear mass dependence. The protons and antiprotons as well as hyperons (Ξ, Ω) spectra have a pronounced shoulder-arm shape at low p_T characteristic of radial flow. The results of the model are shown by the dotted ($\kappa_2 = 2.0$ GeV/fm) and solid ($\kappa_3 = 3.0$ GeV/fm) histograms. Introducing the new $J\bar{J}$ loops algorithm and SCF effects in HIJING/B$\bar{B}$ v2.0 results in a significant improvement (relative to the predictions without SCF [7]) in the description of the pion, kaon, and proton spectra at intermediate p_T for both values of κ. Only a qualitative description is obtained at low p_T due to the presence of elliptic (hydro) and radial expansion [13], not included in our model.

The yields and transverse momentum slopes of (multi) strange particles at moderate p_T are still underestimated for the
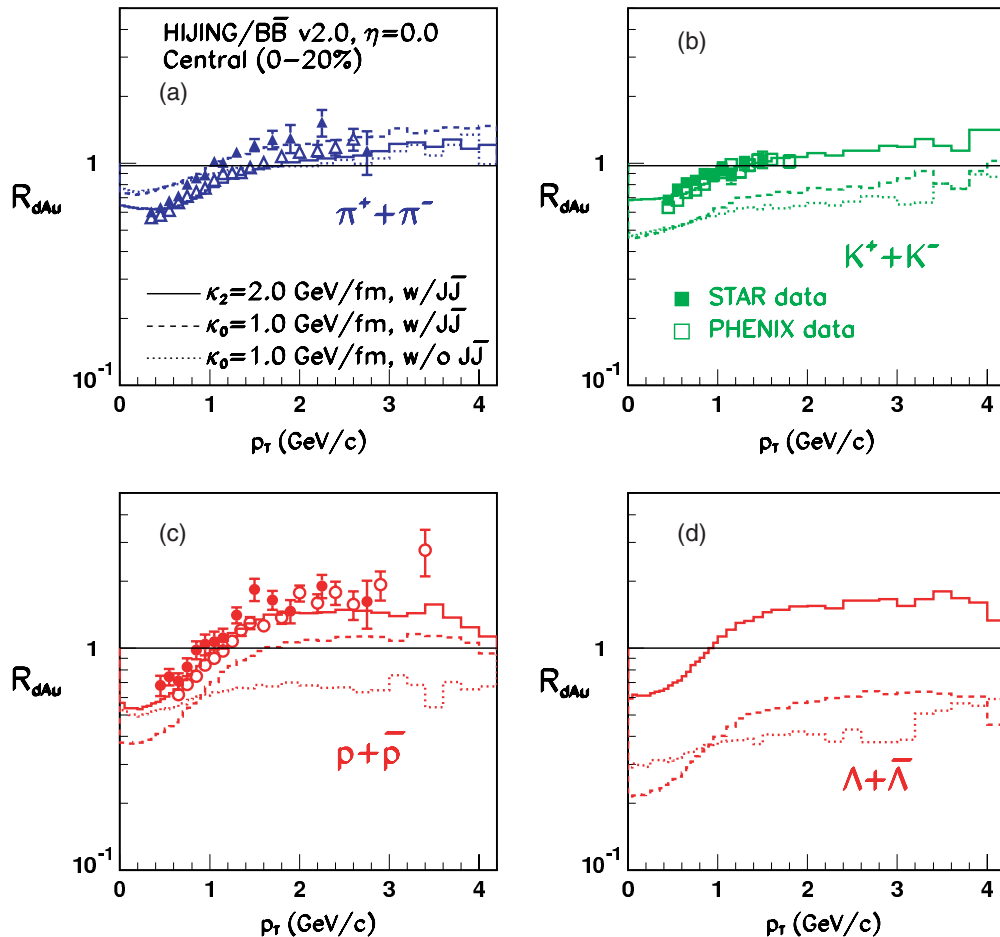
FIG. 8. (Color online) HIJING/B$\bar{\rm B}$ v2.0 predictions for species dependence of nuclear modification factor ($R_{d{\rm Au}}$) in central (0–20%) d+Au collisions at $\sqrt{s_{NN}} = 200$ GeV. Shown are results for (a) charged pions, (b) kaons, (c) inclusive $p+\bar{p}$, and (d) inclusive $\Lambda + \bar{\Lambda}$. The histograms have the same meaning as in right panel of Fig. 5. The data are from STAR (filled symbols) [66] and from PHENIX (open symbols) [72]. Only statistical error bars are shown.

lower value of string tension $\kappa_2 = 2.0$ GeV/fm. Multistrange hyperons yields and spectra, seems to favor the larger value $\kappa_3 = 3.0$ GeV/fm. This suggests that multistrange particles are produced early in the collisions, when temperature is higher than those which characterize the "bulk particles" (i.e., π, K, p). This points towards a dynamical origin and could be explained as an effect of fluctuations of the transient strong color field at early time. Recently, it was also shown that "bulk particles" seem to have a different temperature at kinetic freeze-out than hyperons (Ξ, Ω) suggesting also that multi-strange baryons do not take part in "*the same collectivity*" as π, K, and p during the collision [94,95].

B. Nuclear modification factors

To evaluate if this version of HIJING/B$\bar{\rm B}$ describes the produced entropy, the predicted transverse momentum spectra (left panels) and $R_{d{\rm Au}}$ (right panels) of the total hadron yield for central (0–20%) d+Au collisions, are compared to data from Refs. [63,78] in Fig. 5. The data could not be well described by assuming only a broadening of the *intrinsic k_T* from its standard value $\sigma_{\rm qq} = 0.360$ GeV/c (dotted

histograms) to $\sigma'_{\rm qq} = 1.08$ GeV/c (i.e., including $J\bar{J}$ loops, dashed histograms). The introduction of SCF has a slight effect on the predicted nuclear modification factors $R_{d{\rm Au}}$, but results in a somewhat better agreement with data (solid histograms). Similar results are obtained for minimum bias data. The data indicate at most a small variation with centrality of the factor f consistent with the broadening originating at the parton level.

A slight discrepancy is seen in the description of observed p_T spectra at midrapidity for total inclusive charged hadrons yields in central (0–20%) d+Au collisions. In order to understand this, we analyse charged hadron asymmetries (i.e., the ratio of the hadron yield in backward rapidity to forward rapidity intervals) as proposed in Ref. [96]. Since this observable is defined as a ratio, it is important to check the results for both numerator and denominator. Figure 6 presents the yields in different pseudorapidity interval, backward (a) and forward (b), obtained within HIJING/B$\bar{\rm B}$ v2.0 and HIJING models. The absolute p_T distributions are better described by HIJING/B$\bar{\rm B}$ in comparison to the results of regular HIJING.

In Fig. 7, we analyze the observed charged hadron asymmetries within both models for central (0–20%) and minimum
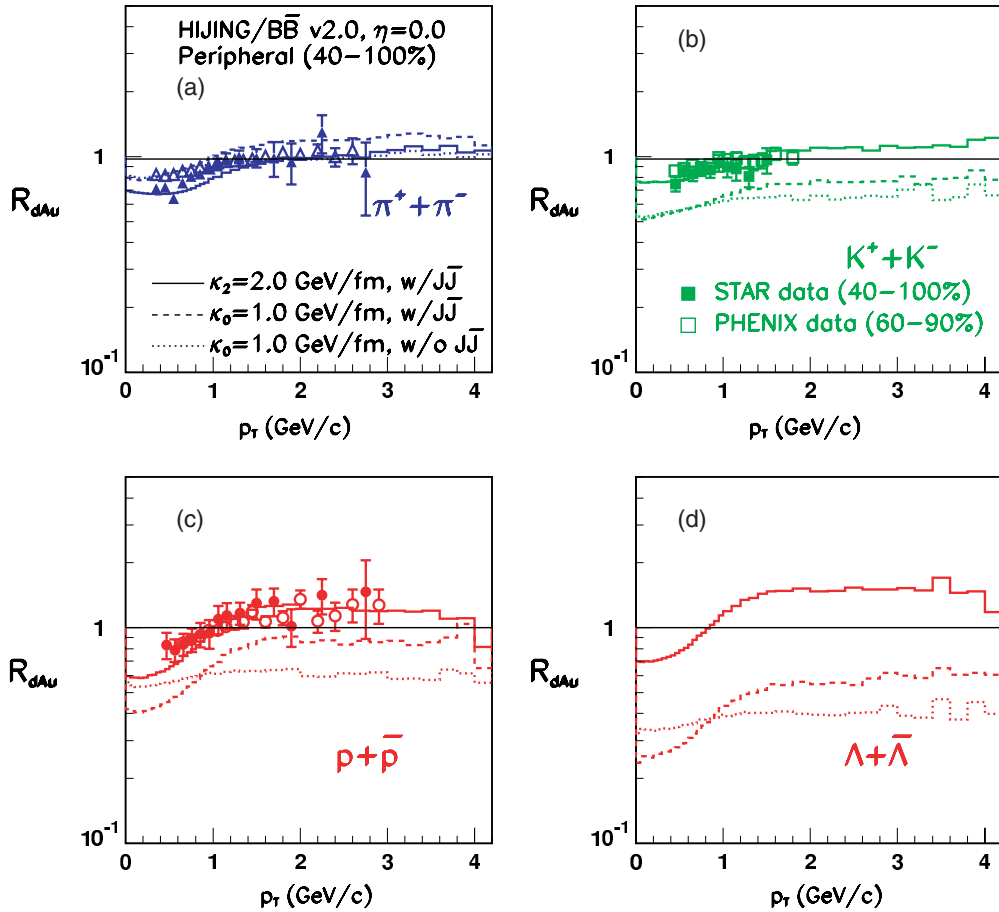
FIG. 9. (Color online) R_{dAu} for peripheral (40–100%) d+Au collisions at $\sqrt{s_{NN}} = 200$ GeV. The histograms have the same meaning as in right panel of Fig. 5. The data are from STAR (filled symbols) [66] and from PHENIX (open symbols) [72]. Only statistical error bars are shown.

bias d+Au collisions. HIJING/B$\bar{\text{B}}$ and HIJING models predict similar asymmetries. The calculated asymmetries are greater than 1.0, in qualitative agreement with the observations and contrary to pQCD predictions [97]. Within our model, the results on asymmetry are also little sensitive to the strength of the assumed longitudinal chromoelectric field. For central (0–20%) d+Au collisions, increasing string tension results in a decrease of the absolute yield (see Fig. 6), without changing the asymmetry significantly. There are still some differences between the p_T dependence of the predicted and measured asymmetry. A relatively good agreement is obtained for minimum bias d+Au collisions in the region $(0.0 < |\eta| < 0.5)$, not shown here. This observable is very delicate and great care should be taken on its interpretation. Our main conclusion is that the small asymmetry is not well reproduced by either models. These observed differences may be related also to the disagreement in the calculated p_T spectra of identified particles for central d+Au collisions discussed above (Sec. III A).

Higher sensitivity to the new dynamics implemented in the HIJING/B$\bar{\text{B}}$ v2.0 is obtained by study of nuclear modification factors of identified particles. To better quantify possible effects of strong color field on particle production, results of $R_{dAu}(p_T)$ for central ($\langle N_{\text{bin}} \rangle = 14.8$) d+Au collisons where

higher sensitivity to SCF is expected, are presented in Fig. 8. Because of their dominance, the production of pions is only moderately modified when we assume an increase of the string tension value since the total energy is conserved. Taking into account SCF effects (solid histograms) results in changes at moderate p_T of $\approx$15–20% of the predicted pion yield (Fig. 8(a)). The pions yield in central d+Au collisions is enhanced relative to p+p collisions (i.e., $R^{\pi}_{dAu}(p_T) > 1$) an effect reproduced by our calculation. The scaling behavior of sum of protons and antiprotons (p+$\bar{p}$) is somewhat different than that of the pions. The (anti)protons are much more sensitive to $J\bar{J}$ loops and SCF effects, and as a result $R^{(p+\bar{p})}_{dAu}(p_T)$ is predicted to be higher than that of pions at moderate p_T. This result is consistent with the data of Ref. [65], where this behavior was explained by different Cronin enhancement for pions and protons. However, within our model it is not only the "Cronin effect" which modified R_{dAu}, but an interplay of initial state effects with an important contribution coming from $J\bar{J}$ loops and SCF. In contrast to pions, (multi)strange particles show a high sensitivity to the presence of SCF. Kaons (Fig. 8(b)) and lambda particles (Fig. 8(d)), show an increase at moderate p_T by a factor of approximately 1.5 and 3.0, respectively, relative to the calculation that do not include $J\bar{J}$ loops and SCF effects
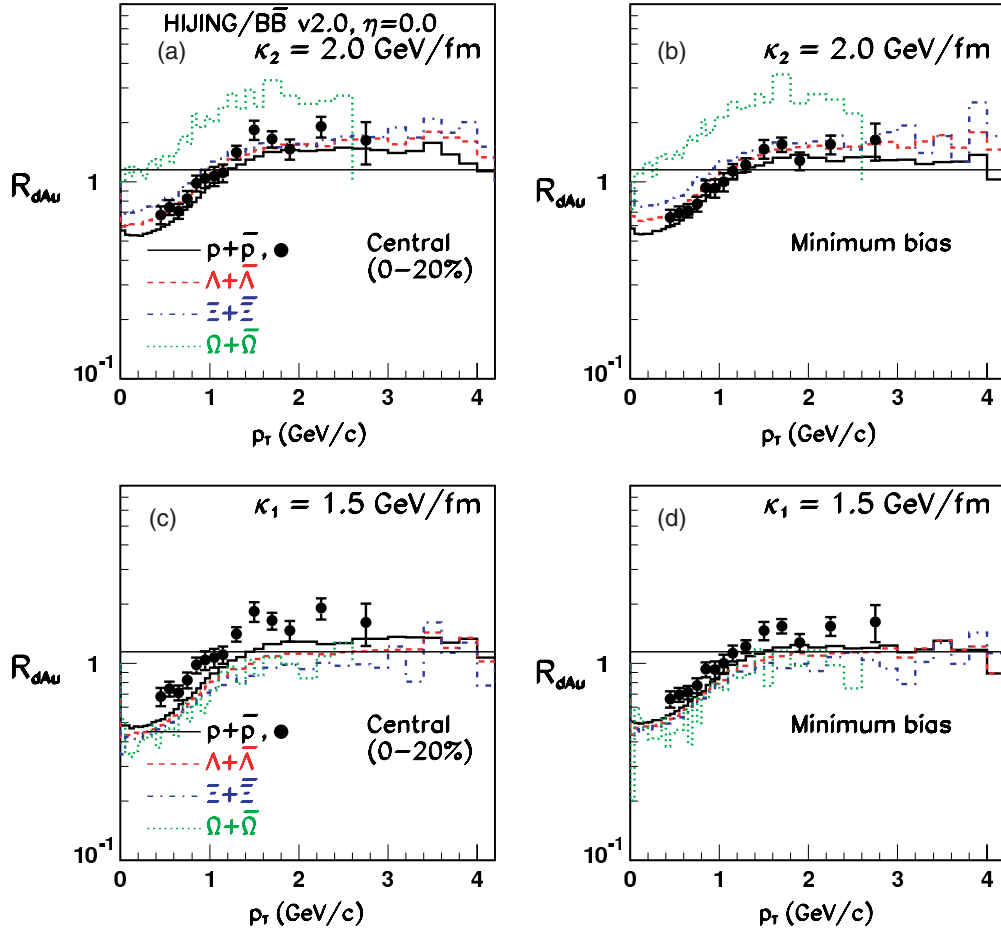
FIG. 10. (Color online) HIJING/B$\bar{\text{B}}$ v2.0 predictions including SCF with $\kappa_2 = 2.0$ GeV/fm (Table II, set 4) (upper panels) and with $\kappa_1 = 1.5$ GeV/fm (Table II, set 3) (lower panels) for central (0–20%) (left panels) and minimum bias (right panels) d+Au collisions at $\sqrt{s_{NN}} = 200$ GeV. Shown are results for inclusive $p+\bar{p}$ (solid), inclusive $\Lambda + \bar{\Lambda}$ (dashed), $\Xi^+ + \Xi^-$ (dash-dotted), and $\Omega^+ + \Omega^-$ (dotted histograms). The data are from STAR [66]. Only statistical error bars are shown.

(dotted histograms). As opposed to pions such an increase results in a predicted strong enhancement of the lambda yield relative to scaled binary collisions.

Figure 9 presents the values of $R_{d\text{Au}}$ for peripheral (40–100%) collisions, where the mean number of collisions is very small, $\langle N_{\text{bin}} \rangle = 4.5$. Our calculations shows that SCF effects play an important role already when there is only a few number of binary collisions. The calculation including SCF describe well the experimental results.

The sensitivity to transient field fluctuations is shown in Fig. 10 which present the predicted $R_{d\text{Au}}(p_T)$ assuming $\kappa_2 = 2.0$ GeV/fm and $\kappa_1 = 1.5$ GeV/fm for central (0–20%) d+Au collisions. For $\kappa_1 = 1.5$ GeV/fm the calculation predicts a value of $R_{d\text{Au}}$ close to one and that decrease somewhat with the mass and strangeness content. Increasing κ to $\kappa_2 = 2.0$ GeV/fm results in a larger enhancement relative to $p+p$ (i.e., $R_{d\text{Au}} > 1$) and a reversing of the order of the nuclear modification factor as a function of the mass and strangeness content. In particular, the model predicts an enhancement in the multistrange (anti)hyperon production at moderate p_T, by a factor of roughly 2 relative to binary scaling for Ξs

and by a factor of approximately 3 for Ωs. Preliminary data on hyperons Λ and Ξ [21,99], seem to favor $\kappa_1 = 1.5$ GeV/fm. However, due to large statistics and systematics error, no clear conclusion could be drawn. Measurements of Ω particles could help us to draw a final conclusion on the importance of SCF fluctuations at top RHIC energy and to determine the effective value (κ) of string tension, in d+Au collisions.

We show in Sec. III A, that a new parametrization of the $p+p$ interaction is necessary to describe the identified particle spectra especially for strange and multistrange particles. This parametrization is different than that of PYTHIA mainly in assuming different constituent and current quark masses for diquark. Therefore the strength of SCF (and κ) introduced in our previous work [8] to best described R_{AuAu} has to be modified because of this new $p+p$ baseline. Figure 11 shows the sensitivity of NMF R_{AuAu} to transient color field fluctuations for the $p+\bar{p}$ yield and for (multi)strange particles. The results assuming $\kappa = \kappa_2 = 2.0$ GeV/fm and $\kappa = \kappa_3 = 3.0$ GeV/fm are shown for both central (0–5%) and peripheral (60–90%) Au+Au collisions. In agreement with the data, the
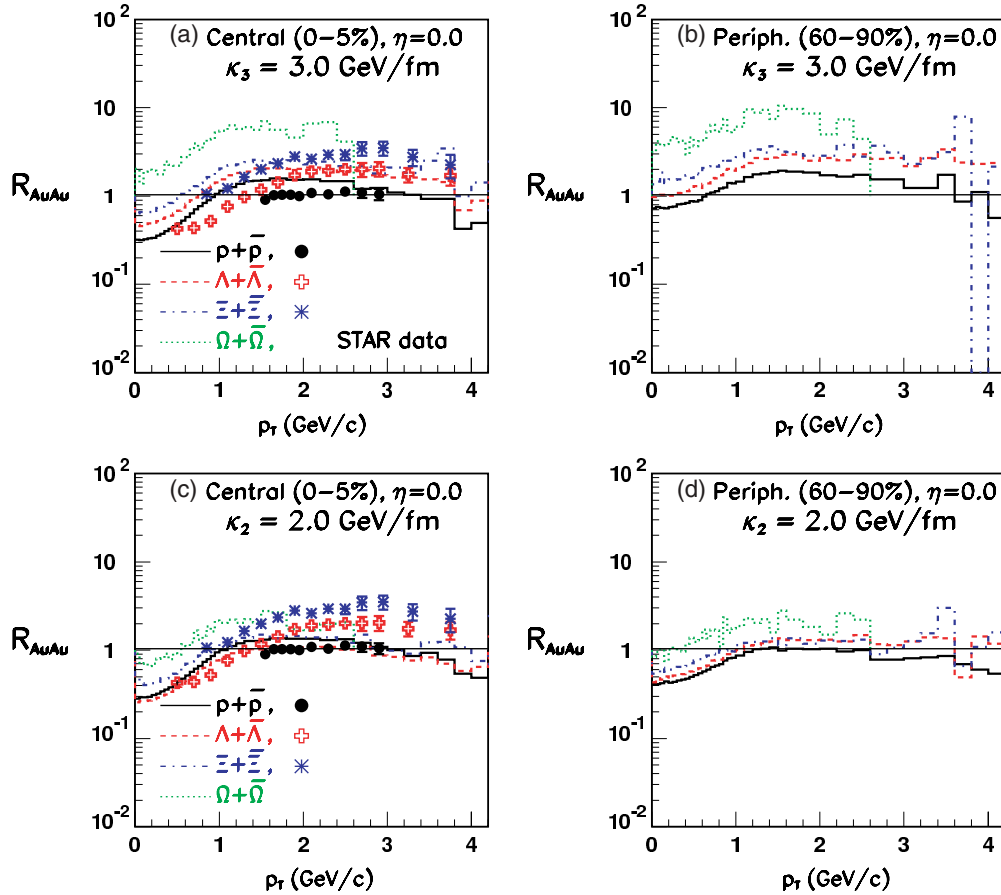
FIG. 11. (Color online) HIJING/B$\bar{\text{B}}$ v2.0 predictions including SCF with $\kappa_3 = 3.0$ GeV/fm (Table II, set 5) (upper panels), and with $\kappa_2 = 2.0$ GeV/fm (Table II, set 4) (lower panels), for central (0–5%) (left panels) and peripheral (60–90%) (right panels) Au+Au collisions at $\sqrt{s_{NN}} = 200$ GeV. The histograms have the same meaning as in Fig. 10. The data are from STAR [66,67,71]. Only statistical error bars are shown.

calculated $p+\bar{p}$ yield scale approximately with the number of binary collisions. In contrast, the observed R_{AuAu} for (multi)strange particles show an enhancement over $p+\bar{p}$, which increase with the mass and strangeness content. A good description of NMF R_{AuAu} for (multi)strange at moderate p_T, is obtained only for the largest value of κ, i.e., κ_3 (Fig. 11(a)). A clear ordering with strangeness content, seen in the data, is not reproduced by lower value $\kappa = \kappa_2 = 2.0$ GeV/fm (Fig. 11(c)). This clearly illustrates that in Au+Au collisions, fluctuations of the chromoelectric field are higher than in d+Au collisions, and affect especially (multi)strange particle yields. The p, π^+, K^+, and their antiparticles are less affected and their yield could also be well described with $\kappa = \kappa_2 = 2.0$ GeV/fm (see also Figs. 4(a) and 4(b)). One note that very similar enhancements are predicted for central and peripheral collisions, with slightly higher value predicted for peripheral (60–90%) collisions, that could be attributed to different strength of quenching effect.

In contrast to R_{AuAu}, R_{CP} obtained as scaled ratios of central (0–5%) and peripheral (60–90%) Au+Au collisions show for (multi)strange particles a slight suppression relative to binary collisions scaling (R_{CP}), see Figs. 3(b) and 3(d) in Ref. [8]. This suppression is mainly due to a final state effect, "jet

quenching," which is stronger in central than in peripheral collisions. A striking difference between R_{AuAu} and R_{CP} has been reported by STAR [21]. This experimental fact could be explained in our model as a consequence of interplay of initial and final state effects. Baryon junction loops ($J\bar{J}$) and SCF effects are taken into consideration in both central and peripheral collisions. In $p+p$ collisions the contribution of junction loops ($J\bar{J}$) is negligible (due to small probability and kinematical cuts), and SCF have a reduced strength ($\kappa_1 = 1.5$ GeV/fm). This show that there could be a significant difference in the value and the meaning of R_{CP} and R_{AuAu} due to differences in the baseline used for comparison with binary scaling, i.e., peripheral (Au+Au) yields for R_{CP} and $p+p$ yields for R_{AuAu}.

IV. SUMMARY AND CONCLUSIONS

We studied the influence of possible multigluon dynamics (*gluon junctions*) and strong longitudinal color fields (SCF) on particle production in heavy-ion collisions. A new parametrization of the $p+p$ interaction based on new constituent and current quark masses for diquark is introduced.

It leads to a simultaneously good description of nonstrange and strange sector in $p+p$ collisions. We show that $J\bar{J}$ loops play an important role in particle production at midrapidity in $d+$Au and Au+Au colisions at RHIC energies. Introducing a new $J\bar{J}$ loops algorithm in the framework of HIJING/B$\bar{\text{B}}$ v2.0, leads to a consistent and significant improvement in the description of the recent experimental results for protons, pions, and kaons for both reactions. The present studies within our model are limited to the effect of initial state baryon production via possible junction dynamics in strong fields. It would be very interesting to consider a generalization of back reaction effects [50] to the case not only of pair production relevant for mesons but to the more difficult three string junction configurations needed to describe baryon production. Baryon productions via the conventional default quark-diquark mechanisms in the Lund string model are known to be inadequate even in $e^+ + e^-$ phenomenology. This is one of the main reasons for our continued exploration of baryon junction alternative mechanisms.

The strange and multistrange particles could only be described in the framework of string models if we consider SCF effects. The mechanisms of their production is very sensitive to the early phase of nuclear collisions, when fluctuations in the color field strength are highest. Within HIJING/B$\bar{\text{B}}$ v2.0, SCF effects are modeled by varying the effective string tension that controls the $q\bar{q}$ and qq$\overline{\text{qq}}$ pair creation rates and strangeness suppression factors. The mid-rapidity yield of (multi)strange particles favor a large value of the average string tension for both collisions (i.e., $\kappa \approx 2.0$ GeV/fm in $d+$Au, and $\kappa \approx 3.0$ GeV/fm in Au+Au). A strong enhancement in strange baryon nuclear modification factors R_{AA} with increasing strangeness content is predicted for $d+$Au and Au+Au. In contrast, a clear ordering with strangeness content is not predicted for lower mean values of string tension.

A greater sensitivity to SCF effects is predicted for the nuclear modification factors of multistrange hyperons Ξ and Ω. In particular, the measurement of Ω and $\bar{\Omega}$ yields would provide an important test of the relevance of SCF fluctuations, helping us to choose appropriate values for the suppression factors γ_Q (where Q = qq, us, s, u), which have strong dependence on the main parameters of QCD (the constituent and current quark masses) and on the system size. Even though the success of this procedure has been clearly illustrated here, the full understanding of the production of (multi) strange particles in relativistic heavy-ion collisions remain an exciting open question, and challenge many theoretical ideas.

APPENDIX: TABLES

TABLE I. Main parameters used in the calculation for $p+p$ collisions. The parameters are defined in the text. Set 1 is used in PYTHIA (and regular HIJING). Set 2 is obtained using the constituent quark masses from Sec. II B. Set 3 includes an additional increase of the string tension to $\kappa_1 = 1.5$ GeV/fm.

$p+p$	κ (GeV/fm)	γ_{qq}	γ_s	γ_{us}	γ_{10}	σ_q (GeV/c)	f
Set 1	$\kappa_0 = 1.0$	0.09	0.30	0.40	0.05	0.350	1
Set 2	$\kappa_0 = 1.0$	0.02	0.30	0.40	0.05	0.350	1
Set 3	$\kappa_1 = 1.5$	0.07	0.45	0.54	0.09	0.430	1

TABLE II. Main parameters used in $d+$Au and Au+Au collisions. The parameters are defined in the text. Set 1 correspond to calculations without $J\bar{J}$ loops and SCF effects. Set 2 adds the contribution of $J\bar{J}$ loops. Sets 3–5 include both effects and correspond to different values of the string tension.

(d) Au+Au	κ (GeV/fm)	γ_{qq}	γ_s	γ_{us}	γ_{10}	σ_q (GeV/c)	f
Set 1	$\kappa_0 = 1.0$	0.02	0.30	0.40	0.05	0.350	1
Set 2	$\kappa_0 = 1.0$	0.02	0.30	0.40	0.05	0.350	3
Set 3	$\kappa_1 = 1.5$	0.07	0.45	0.54	0.09	0.430	3
Set 4	$\kappa_2 = 2.0$	0.14	0.55	0.63	0.12	0.495	3
Set 5	$\kappa_3 = 3.0$	0.27	0.67	0.74	0.18	0.606	3

[1] PHENIX Collaboration, K. Adcox *et al.*, Phys. Rev. Lett. **89**, 092302 (2002).
[2] PHENIX Collaboration, S. S. Adler *et al.*, Phys. Rev. Lett. **91**, 172301 (2003).
[3] I. Vitev and M. Gyulassy, Phys. Rev. C **65**, 041902(R) (2002).
[4] M. Gyulassy, I. Vitev, X.-N. Wang, and B. W. Zhang, in *Quark Gluon Plasma 3*, edited by R. C. Hwa and X.-N. Wang (World Scientific, Singapore, 2003), pp. 123–191.
[5] PHENIX Collaboration, K. Adcox *et al.*, Phys. Rev. Lett. **88**, 022301 (2002).

[6] PHENIX Collaboration, G. David *et al.*, Nucl. Phys. **A698**, 227 (2002).
[7] V. Topor Pop, M. Gyulassy, J. Barrette, C. Gale, X.-N. Wang, and N. Xu, Phys. Rev. C **70**, 064906 (2004), and references therein.
[8] V. Topor Pop, M. Gyulassy, J. Barrette, and C. Gale, Phys. Rev. C **72**, 054901 (2005).
[9] D. Kharzeev, Phys. Lett. **B378**, 238 (1996).
[10] R. J. Fries, B. Muller, C. Nonaka, and S. A. Bass, Phys. Rev. C **68**, 044902 (2003); V. Greco, C. M. Ko, and P. Levai,

Phys. Rev. Lett. **90**, 202302 (2003); R. C. Hwa and C. B. Yang, Phys. Rev. C **70**, 024905 (2004).

[11] M. Grabiak, J. A. Casado, and M. Gyulassy, Z. Phys. C **49**, 283 (1991).

[12] T. S. Biro, B. Müller, and X.-N. Wang, Phys. Lett. **B283**, 171 (1992).

[13] P. F. Kolb and U. Heinz, in Quark Gluon Plasma 3, edited by R. C. Hwa and X.-N. Wang (World Scientific, Singapore, 2003), pp. 634–714.

[14] T. S. Biro, H. B. Nielsen, and J. Knoll, Nucl. Phys. **B245**, 449 (1984).

[15] S. Soff, J. Phys. G **30**, S139 (2004); S. Soff, J. Randrup, H. Stoecker, and N. Xu, Phys. Lett. **B551**, 115 (2003); S. Soff, S. Kesavan, J. Randrup, H. Stoecker, and N. Xu, J. Phys. G **30**, L35 (2004).

[16] R. J. Fries, J. I. Kapusta, and Y. Li, Nucl. Phys. **A774**, 861 (2006).

[17] T. Lappi and L. McLerran, Nucl. Phys. **A772**, 200 (2006).

[18] M. Asakawa, S. A. Bass, and B. Müller, Phys. Rev. Lett. **96**, 252301 (2006).

[19] G. Ripka, hep-ph/0310102, Lectures delivered at European Center for Theoretical Studies in Nuclear Physics and Related Areas, 2002-2003, ECT, Trento, Italy; Berlin, Germany: Springer (2004), p 138 (Lecture Notes in Physics, 639).

[20] J. Rafelski and B. Müller, Phys. Rev. Lett. **48**, 1066 (1982); **56**, 2334 (1986); H. Z. Huang and J. Rafelski, AIP Conf. Proc. No. **756**, 210 (2005).

[21] R. Bellwied, J. Phys. G **30**, S29 (2004).

[22] Helen Caines (for the STAR Collaboration), J. Phys. G **31**, S1057 (2005).

[23] C. Greiner, J. Phys. G **28**, 1631 (2002).

[24] N. Armesto, M. A. Braun, E. C. Ferreiro, and C. Pajares, Phys. Lett. **B344**, 301 (1995); N. Armesto, M. A. Braun, E. C. Ferreiro, C. Pajares, and Yu. M. Shabelski, *ibid.* **B389**, 78 (1996).

[25] Tai An and Sa Ben-Hao, Phys. Lett. **B409**, 393 (1997).

[26] V. K. Magas, L. P. Csernai, and D. D. Strottman, Phys. Rev. C **64**, 014901 (2001).

[27] S. E. Vance and M. Gyulassy, Phys. Rev. Lett. **83**, 1735 (1999).

[28] S. E. Vance, J. Phys. G **27**, 603 (2001).

[29] The updated FORTRAN sources of the program can be downloaded from URL address http://www.physics.mcgill.ca/~toporpop/bb21_aug2006.

[30] X.-N. Wang and M. Gyulassy, Phys. Rev. D **44**, 3501 (1991); M. Gyulassy and X.-N. Wang, Comput. Phys. Commun. **83**, 307 (1994); X.-N. Wang, Phys. Rep. **280**, 287 (1997).

[31] T. Sjöstrand, Comput. Phys. Commun. **82**, 74 (1994).

[32] V. Topor Pop, M. Gyulassy, J. Barrette, C. Gale, X.-N. Wang, N. Xu, and K. Filimonov, Phys. Rev. C **68**, 054902 (2003).

[33] S. E. Vance, M. Gyulassy, and X.-N. Wang, Phys. Lett. **B443**, 45 (1998).

[34] STAR Collaboration, J. Adams *et al.*, Phys. Rev. Lett. **95**, 122301 (2005).

[35] P. D. Collins, *An Introduction to Regge Theory and High Energy Physics* (Cambridge University Press, Cambridge, 1977), p. 445.

[36] B. Z. Kopeliovich and B. Povh, Phys. Lett. **B446**, 321 (1999).

[37] A. V. Prozorkevich, S. A. Smolyansky, V. V. Skokov, and E. E. Zabrodin, Phys. Lett. **B583**, 103 (2004).

[38] V. V. Skokov and P. Levai, Phys. Rev. D **71**, 094010 (2005).

[39] S. Soff, S. A. Bass, M. Bleicher, L. Bravina, E. Zabrodin, H. Stöcker, and W. Greiner, Phys. Lett. **B471**, 89 (1999).

[40] G. E. Brown and M. Rho, Phys. Rev. Lett. **66**, 2720 (1991).

[41] M. Bleicher, W. Greiner, H. Stoecker, and N. Xu, Phys. Rev. C **62**, 061901 (2000).

[42] J. Schaffner-Bielich, J. Phys. G **30**, R245 (2004).

[43] S. B. Rüster, V. Werth, M. Buballa, I. A. Shovkovy, and D. H. Rischke, Phys. Rev. D **72**, 034004 (2005).

[44] D. Kharzeev and K. Tuchin, Nucl. Phys. **A753**, 316 (2005).

[45] A. Casher, H. Neuberger, and S. Nussinov, Phys. Rev. D **20**, 179 (1979); **21**, 1966 (1980).

[46] J. S. Schwinger, Phys. Rev. **82**, 664 (1951).

[47] G. C. Nayak and P. van Nieuwenhuizen, Phys. Rev. D **71**, 125001 (2005); G. C. Nayak, *ibid.* **72**, 125010 (2005); F. Cooper and G. C. Nayak, *ibid.* **73**, 065005 (2006).

[48] H. Gies and K. Klingmüller, Phys. Rev. D **72**, 065001 (2005).

[49] H. M. Fried and Y. Gabellini, Phys. Rev. D **73**, 011901(R) (2006).

[50] Y. Kluger, J. M. Eisenberg, B. Svetitsky, F. Cooper, and E. Mottola, Phys. Rev. D **45**, 4659 (1992); Y. Kluger, J. M. Eisenberg, B. Svetitsky, F. Cooper, and E. Mottola, Phys. Rev. Lett. **67**, 2427 (1991); Y. Kluger, E. Mottola, and J. M. Eisenberg, Phys. Rev. D **58**, 125015 (1998).

[51] F. Cooper, E. Mottola, and G. C. Nayak, Phys. Lett. **B555**, 181 (2003).

[52] E. Eidelman *et al.* (Particle Data Group), Phys. Lett. **B592**, 1 (2004).

[53] M. Cristoforetti, P. Faccioli, G. Ripka, and M. Traini, Phys. Rev. D **71**, 114010 (2005).

[54] N. S. Amelin, N. Armesto, C. Pajares, and D. Sousa, Eur. Phys. J. C **22**, 149 (2001).

[55] W. Florkowski, Acta Phys. Pol. B **35**, 799 (2004).

[56] S. Steinke and J. Rafelski, J. Phys. G **32**, S455 (2006).

[57] G. Hooft, hep-th/0408148, presented at the Workshop on Hadrons and Strings, Trento, July (2004); published in Trento 2004, "Large N(c) QCD," pp. 1–13.

[58] G. Martens, C. Greiner, S. Leupold, and U. Mosel, Phys. Rev. D **70**, 116010 (2004).

[59] T. T. Takahashi, H. Matsufuru, Y. Nemoto, and H. Suganuma, Phys. Rev. Lett. **86**, 18 (2001); T. T. Takahashi, H. Suganuma, Y. Nemoto, and H. Matsufuru, Phys. Rev. D **65**, 054503 (2002); F. Okiharu, H. Suganuma, and T. T. Takahashi, *ibid.* **72**, 014505 (2005).

[60] D. d'Enteria, J. Phys. G **31**, S491 (2005).

[61] STAR Collaboration, J. Adams *et al.*, Phys. Rev. Lett. **91**, 172302 (2003).

[62] PHENIX Collaboration, S. S. Adler *et al.*, Phys. Rev. Lett. **91**, 241803 (2003).

[63] STAR Collaboration, J. Adams *et al.*, Phys. Rev. Lett. **92**, 112301 (2004).

[64] STAR Collaboration, J. Adams *et al.*, Phys. Rev. Lett. **92**, 052302 (2004).

[65] STAR Collaboration, J. Adams *et al.*, Phys. Lett. **B616**, 8 (2005).

[66] STAR Collaboration, J. Adams *et al.*, Phys. Lett. **B637**, 161 (2006).

[67] STAR Collaboration, B. I. Abelev *et al.*, nucl-ex/0607033 (submitted to Phys. Rev. C).

[68] STAR Collaboration, R. Bellwied *et al.*, nucl-ex/0511006v2 (to be published in Acta Phys. Hung. A).

[69] PHENIX Collaboration, S. S. Adler *et al.*, Phys. Rev. C **69**, 034910 (2004).

[70] STAR Collaboration, J. Adams *et al.*, Nucl. Phys. **A757**, 102 (2005).

[71] STAR Collaboration, J. Adams *et al.*, nucl-ex/0606014 (submitted to Phys. Rev. Lett.).

[72] PHENIX Collaboration, S. S. Adler *et al.*, Phys.Rev. C **74**, 024904 (2006).

[73] T. Alexopoulos *et al.*, Phys. Lett. **B435**, 453 (1998).

[74] PHENIX Collaboration, S. S. Adler *et al.*, Phys. Rev. D **74**, 072002 (2006).

[75] R. P. Feynman, R. D. Field, and G. C. Fox, Nucl. Phys. **B128**, 1 (1977).

[76] B. Kniehl, G. Kramer, and B. Potter, Nucl. Phys. **B597**, 337 (2001).

[77] PHENIX Collaboration, S. S. Adler *et al.*, Phys. Rev. Lett. **91**, 072303 (2003).

[78] STAR Collaboration, J. Adams *et al.*, Phys. Rev. Lett. **91**, 072304 (2003).

[79] BRAHMS Collaboration, I. Arsene *et al.*, Phys. Rev. Lett. **91**, 072305 (2003).

[80] PHOBOS Collaboration, B. B. Back *et al.*, Phys. Rev. Lett. **91**, 072302 (2003).

[81] J. W. Cronin *et al.*, Phys. Rev. D **11**, 3105 (1975).

[82] D. Antreasyan *et al.*, Phys. Rev. D **19**, 764 (1979).

[83] G. Papp, P. Levai, and G. Fai, Phys. Rev. C **61**, 021902(R) (1999).

[84] X.-N. Wang, Phys. Rev. C **61**, 064910 (2000).

[85] I. Vitev and M. Gyulassy, Phys. Rev. Lett. **89**, 252301 (2002).

[86] A. Accardi and M. Gyulassy, Phys. Lett. **B586**, 244 (2004).

[87] R. Vogt, Phys. Rev. C **70**, 064902 (2004).

[88] N. Armesto, J. Phys. G **32**, R367 (2006).

[89] D. Kharzeev, E. Levin, and L. McLerran, Phys. Lett. **B561**, 93 (2003).

[90] R. C. Hwa, C. B. Yang, and R. J. Fries, Phys. Rev. C **71**, 024902 (2005).

[91] M. Gyulassy and P. Levai, Phys. Lett. **B442**, 1 (1998).

[92] Z.-W. Lin and C. M. Ko, Phys. Rev. C **68**, 054904 (2003).

[93] K. Werner, F. M. Liu, and T. Pierog, Phys. Rev. C **74**, 044902 (2006).

[94] STAR Collaboration, M. Estienne *et al.*, J. Phys. G **31**, S873 (2005).

[95] N. Xu, J. Phys. G **32**, s123 (2006).

[96] STAR Collaboration, J. Adams *et al.*, Phys. Rev. C **70**, 064907 (2004).

[97] X. N. Wang, Phys. Lett. **B565**, 116 (2003).

[98] STAR Collaboration, R. Bellwied *et al.*, J. Phys. G **31**, S675 (2005).

[99] Camelia Mironov (for the STAR Collaboration), J. Phys. G **31**, S1195 (2005).